EEET ECOLOGICAL ENGINEERING & ENVIRONMENTAL TECHNOLOGY

Ecological Engineering & Environmental Technology 2024, 25(11), 146–162
https://doi.org/10.12912/27197050/192970
ISSN 2299–8993, License CC-BY 4.0

Received: 2024.08.22
Accepted: 2024.09.15
Published: 2024.10.01

Hybrid Modelling Using Lattice Boltzmann and Finite Difference Methods of Dikes Effect on Sediment Transport and Morphological Processes with a Quasi-Tridimensional Approach

Khalil Machrouhi[1], Anass Bendaraa[1*], My Mustapha Charafi[1], Abdellatif Hasnaoui[1]

[1] LS2ME Polydisciplinary Faculty of Khouribga, Sultan Moulay Slimane University BP: 145, 25000, Morocco

* Corresponding author's e-mail: anass.bendaraa@gmail.com

ABSTRACT

This paper presents the development of a quasi-three-dimensional model that utilizes an equilibrium technique to investigate the morphological change of a channel focused on transport of sediment. The authors developed a computational algorithm that integrates two numerical techniques, specifically the Lattice Boltzmann Method (LBM) and the finite-difference method (FDM), to perform a hybrid calculation. The aforementioned algorithm was employed to investigate the impact of dykes on the dynamics of channel flow, sediment transport, and bed evolution. To derive the three-dimensional velocity field, the Boltzmann lattice method is employed to compute the two horizontal components of the vertically integrated velocity. Subsequently, these two components are combined with a logarithmic vertical profile. The process of sediment particle transport can be divided into two components: the bed load transport rate and the suspended load transport rate. The latter determination is achieved through the computation of the equilibrium flow rate of suspended sediment, which is derived from the equilibrium concentrations and logarithmic velocities. by comparing its outputs to previous research on constant width channels and horizontal beds, especially in dykes, the model was validated. This model accurately predicts sediment transport as bed load and suspended load, which is important for understanding sediment dynamics around such structures. the model's ability to anticipate sediment erosion and deposition across the channel, providing crucial insights into river detours and other sedimentary processes.

Keywords: sediment transport, shallow-water flow, dykes, channel morphology, Lattice Boltzmann method, finite difference method.

INTRODUCTION

The examination of sediment circulation procedures includes the dynamics of rock movement within an area of mountains, as well as the chemical diffusion of materials in water, alongside various other processes. The primary objective of this study is to investigate the transportation of sediments that occurs as a result of hydrodynamic processes in aquatic environments.

The precise estimation of sediment transport rates holds significant importance in the field of morphological research pertaining to river, coastal, and marine settings. In the present setting, numerous studies have been conducted to forecast the patterns of fluid dynamics in different structures (Zhou, 2002; Cai et al., 2007; Zhang et al., 2021). The hydrodynamic aspect is represented by the Shallow Water equations, which are employed to analyze the flow of fluid in rivers, channels, coastal regions, and similar locations. The morphodynamic aspect is handled by an equation for sediment transport, which takes into account the movement of solid particles.

Human interventions, such as the construction of dams or ports, profoundly affect natural systems, making it essential to understand these interactions for effective management and accurate predictive modeling of morphological changes driven by anthropogenic factors. Integrating

flood control strategies with ecosystem conservation efforts is therefore critical. By employing predictive models that simulate different configurations, we can anticipate potential impacts on flood management and ecosystem health. This approach emphasizes understanding the feedback loops between sediment dynamics, flow characteristics, and ecological integrity. Thanks to the advanced development of computer tools, numerical modeling has become an essential tool for predicting phenomena that require expensive resources. Several studies have been carried out in the literature using classical methods such as FDM and finite element methods. (Charafi et al., 2000) have developed a quasi-three-dimensional mathematical model utilizing the FDM to investigate morphological processes. Our model utilizes the equilibrium sediment transport approach. Flow velocities are determined by employing a two-dimensional depth-averaged horizontal flow model (H2D), coupled with logarithmic profiles. The authors in (Charafi et al., 2000) The identical methodologies were employed to replicate the transportation of sediment and pollutants within a shallow basin. The mechanism of sediment particle transport through water flow was examined in terms of two distinct loads: a bottom load and a suspended load. The transport rate of the bed load is characterized as the migration of particles by rolling and saltation processes across the surface of the bed (Adamsson et al., 2003).

Various alternative computer methods, including the finite-element method, finite-volume method, and the finite-difference method, can be employed for the purpose of modeling the mathematical models governing shallow water. See (Hu et al., 2010; Zapata et al., 2021) among others. Far from the classical deterministic methods, the stochastic Boltzmann method, known for its efficiency, speed and ease of application, has rarely been used in the field of free surface flows. Indeed, unlike other fields such as thermofluidic for confined flows (Gawas et al., 2021; Shi et al., 2021; Suzuki et al., 2021; Wen et al., 2022) (cavities, pipes, etc.) where it has been applied in several works, references leading to the modelling of shallow flows using the LBM remain few and far between (Zhou, 2002). Similarly, the general agreement about the utilization of the Lattice Boltzmann approach among researchers has focused on studies other than free-surface flows. (Chen et al., 1998; Aidun et al., 2010; Guo et al., 2013), which shows the interest of the present study.

In these ecosystems, shallow-water flows influence sediment distribution and change. Particles rolling or bouncing along the bottom, or suspended in the water column, move silt in shallow channels. Flow dynamics, such as velocity and depth, have an impact on sediment entrainment and deposition. To simulate these processes, our study uses a combination of a probabilistic method and a deterministic method, specifically the lattice Boltzmann method and the finite difference method. This shows how flow characteristics, bed topography, and sediment distribution all affect each other. This will enrich our library of numerical models, which already includes other models based on deterministic methods such as the finite difference method, the finite element method, and the finite volume methods. Our motivation for choosing the lattice Boltzmann method was its ability to support different Multiphysics couplings, its purely explicit aspect and its good scalability in intensive computing. Likewise, its use in the field of free surface flows is justified by its ability to describe the behavior of incompressible or compressible fluids in flow. By a development of Chapman-Enskog (Benkhaldoun et al., 2007), This phenomenon leads to the first-order Euler equation and the second-order Navier-Stokes equation. This method's primary advantage lies in its ability to characterize several types of fluid dynamics, including free surface flows, flows in complicated media, flows involving heat transfer, and flows of multi-component mixtures.

In the present work, and in order to achieve this objective, the investigation generated a quasi-three-dimensional simulation by integrating the lattice Boltzmann process with the finite-difference approach to study the effect of different obstacle arrangements on the flow and on the evolution of the morphology of the bottom under the effect of erosion, transport and deposition of sediments. The free surface flow study was carried out using the calculation code developed using the LBM method, with flow velocity and water height as output data incorporated into a second calculation code based on FDM is employed to forecast sediment movement and bottom fluctuations in channels of rivers, coasts, or marine areas with a muddy bottom, initially flat and horizontal, and partially blocked by an obstacle. In order to validate the chosen approach, the model was implemented by conducting a comparative analysis of the generated results with those of previous studies, making it possible to validate the present calculation code before embarking on the prediction of the effect of

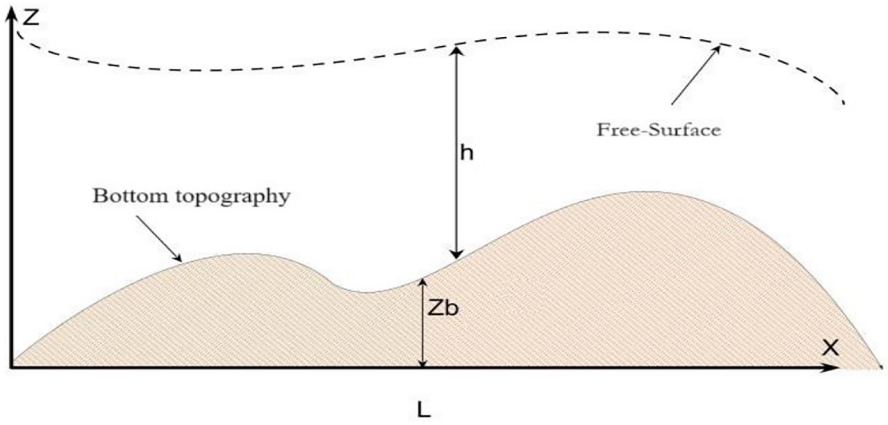

Figure 1. Shallow water flow vertical cross-section schematic

obstacles on the appearance of zones of deposition and/or erosion of sediment, and consequently on the evolution of the channel bed.

The novelty of this work is evident in the creation of a hybrid calculation programs (FDM-LBM) to leverage the benefits of the lattice Boltzmann method in terms of performance, accuracy, and simplicity of implementation, enabling the obtaining of an efficient and effective computer program.

MATHEMATICAL MODEL

Equations of shallow water

In most cases, flows in channels with large horizontal dimensions can be efficiently and accurately described using the Saint-Venant equations known as the (SWE) shallow water equations. Considering the shallow water approximation (SWA), Given the assumption that the depth of flow is significantly smaller in comparison to the conventional scales of horizontal dimensions, the following equations are derived. Given vertical pressure gradient and acceleration of gravity, vertical acceleration is generally supposed to be minimal. Integrating the pressure gradient over the vertical dimension reveals that the pressure is hydrostatic. These approximations allowed Saint-Venant to establish equations that describe mean flow by integrating the three-dimensional Navier-Stokes equations on the vertical (Figure 1).

In this context, The equations governing the conservation of mass (continuity equation) and momentum of the mean flow are expressed as follows (Charafi et al., 2000) (Bernsdorf et al., 1999; Benkhaldoun et al., 2007):

$$\frac{\partial h}{\partial t}+\frac{\partial(h\tilde{u})}{\partial x}+\frac{\partial(h\tilde{v})}{\partial y}=0 \tag{1}$$

$$\frac{\partial(h\tilde{u})}{\partial t}+\frac{\partial\left(h\tilde{u}^2\right)}{\partial x}+\frac{\partial(h\tilde{u}\tilde{v})}{\partial y}=-g\frac{\partial}{\partial x}\left(\frac{1}{2}h^2\right)+\nu\frac{\partial^2(h\tilde{u})}{\partial x\,\partial x}+\nu\frac{\partial^2(h\tilde{v})}{\partial y\,\partial y} -g\frac{\partial z_b}{\partial x}+f_c h\tilde{v}+\frac{\tau_{wx}}{\rho}-\frac{\tau_{bx}}{\rho} \tag{2}$$

$$\frac{\partial(h\tilde{v})}{\partial t}+\frac{\partial(h\tilde{u}\tilde{v})}{\partial x}+\frac{\partial\left(h\tilde{v}^2\right)}{\partial y}=-g\frac{\partial}{\partial x}\left(\frac{1}{2}h^2\right)+\nu\frac{\partial^2(h\tilde{u})}{\partial x\,\partial x}+\nu\frac{\partial^2(h\tilde{v})}{\partial y\,\partial y} -g\frac{\partial z_b}{\partial x}-f_c h\tilde{u}+\frac{\tau_{wy}}{\rho}-\frac{\tau_{by}}{\rho} \tag{3}$$

where: $\tilde{u}$ and $\tilde{v}$ are Formulas for depth-averaged horizontal velocities in x and y directions:

$$\tilde{u}=\frac{1}{h}\int_Z^{h+Z} u dz\,;\ \tilde{v}=\frac{1}{h}\int_Z^{h+Z} v dz \tag{4}$$

Water depth (h), time (t), bed elevation (z_b), gravitational acceleration (g = 9.81m/s^2), water density (ρ), and kinematic viscosity (ν) are the variables. After eliminating the top bars of the previous equations for the sake of simplicity, the continuity Equation 1 and the momentum Equations 2 and 3 can be expressed in the subsequent tensor mathematical form:

$$\frac{\partial h}{\partial t} + \frac{\partial (hu_i)}{\partial x_i} = 0 \tag{5}$$

$$\frac{\partial (hu_i)}{\partial t} + \frac{\partial (hu_i u_j)}{\partial x_j} = -g \frac{\partial}{\partial x_i}\left(\frac{h^2}{2}\right) + \nu \frac{\partial^2 (hu_i)}{\partial x_j \partial x_j} + F_i \tag{6}$$

where: i and j represent indices in accordance with the Einstein summation convention, u_i and u_j Fluid velocity components (m/s). In this convention, repeated indices indicate summing over spatial coordinates. x_i refers to the Cartesian coordinate, while F_i is referred to as the force term. The current study applies the force term as follows:

$$F_i = -g \frac{\partial z_b}{\partial x_i} - \frac{\tau_{bi}}{\rho} \tag{7}$$

The bed shear stress, represented as τ_{bi}, in the direction i is determined by the average velocities at depth, as expressed by the following equation:

$$\tau_{bi} = \rho C_b u_i \sqrt{u_j u_j} \tag{8}$$

where: C_b is the bed friction coefficient, which can be either constant or estimated from $C_b = \frac{g n_b^2}{h^{1/3}}$, where the Manning coefficient for bed level is represented by n_b.

LBM – Lattice-Boltzmann method

Developed recently, the Lattice Boltzmann method is a numerical method that differs from the traditional methods employed in numerical flow simulation. The concept was initially developed in the 90s as a means of addressing lattice gasses and cellular automata. The approach depends on a mesoscopic model of fluid dynamics. It lies between the microscopic and macroscopic scales. Unlike conventional methods, which consider a macroscopic description of the elementary representative volume, LBM is based on statistical physics, The topic under consideration pertains to the numerical resolution of the Boltzmann equation. The present study used a partial differential equation to represent the dynamics of velocity distribution with respect to an external force. This is referred to as a mesoscopic representation of flow motion. By employing a multi-scale analysis, the macroscopic variables (h, u, v) of the flow can be determined through straightforward numerical integration of several moments of different orders (Zhou, 2002).

Boltzmann equation

As mentioned above the Boltzmann equation is a partial differential equation (PDE) that characterizes the temporal evolution of the displacement distribution of a mass particle under the influence of a force that varies with velocity(Brush, 2003).
This equation is given by :

$$\frac{\partial f}{\partial t} + v \cdot \nabla f = \Omega(f) + F \tag{9}$$

where: v is the microscopic speed, Ω indicate the collision word, F considers the influence of external forces.

In fact, this equation reflects two phenomena: particle advection and the effect of collision between particles. In the absence of collisions, the particles are solely propelled by the force's action. The evolutionary trajectory of the system is depending on the specific configuration of the collision operator when particles come into contact. It wasn't until 1954 that Bhatnagar, Gross and Krook (Bhatnagar et al., 1954) proposed a simple model of collision (known as BGK), dependent around the notion that particles collide around an equilibrium distribution and during a time called the relaxation time. With BGK collision, it was demonstrated that the Boltzmann equation This term can be employed to characterize fluid mechanics flows that are regulated by the Navier-Stokes equations.

Discretization – D2Q9 model

The Lattice Boltzmann Method (LBM) comprises two main stages: A stage of propagation and a stage of collision. In accordance with their previous placements and velocities, particles suffer displacement to alternative locations.
The propagation and a collision stage yield the character governed by the following lattice Boltzmann equation:

$$f_\alpha(x + e_\alpha \Delta t, t + \Delta t) - f_\alpha(x, t) = -\frac{1}{\tau}\left(f_\alpha - f_\alpha^{eq}\right) + \frac{\Delta t}{6e^2} e_{\alpha i} F_i \tag{10}$$

where: f_α is the distribution function of a particle, f_α^{eq} is the local equilibrium distribution function defined by Equation 18, $e = \frac{\Delta x}{\Delta t}$ where Δx is lattice size and Δt is the time step, $e_{\alpha i}$ is the i^{th} component of the particle velocity vector e_α in the α = 0,1,2,…,8 link given in Equation 12 (see Figure 2) and τ is the total relaxation time.

Water depth h and velocity components u_i are defined as follows:

$$h = \sum_\alpha f_\alpha \; and \; u_i = \frac{1}{h}\sum_\alpha e_{\alpha i} f_\alpha, \tag{11}$$

It can be proved in theory that the depth h and velocity u_i calculated from the above expressions are solutions to the shallow-water equations (Equations 5 and 6).

The Boltzmann model is based on square lattices, where the 9-speed version (Figure 2) is the most frequently used. It generally gives more accurate results.

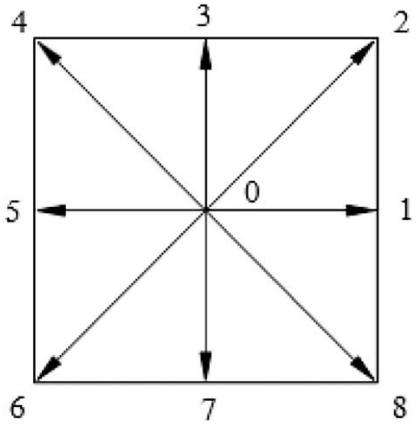

Figure 2. Square lattice (9 – speed)

In the present study, the 9 – velocity square network (D2Q9 model) is used. The particle velocity vector is defined as follows:

$$e_\alpha = \begin{cases} (0,0), & \alpha = 0 \\ e\left[\cos\dfrac{(\alpha-1)\pi}{4}, \sin\dfrac{(\alpha-1)\pi}{4}\right], & \alpha = 1,3,5,7 \\ \sqrt{2}e\left[\cos\dfrac{(\alpha-1)\pi}{4}, \sin\dfrac{(\alpha-1)\pi}{4}\right], & \alpha = 2,4,6,8 \end{cases} \tag{12}$$

As mentioned previously, the collision model used is the one proposed by Bhatnagar Gross and Krook called the BGK model. It is based on a single relaxation time (SRT) and has been proven to be very simple and effective (Zou et al., 1997), (Klar et al., 2008) for simulating fluid flows. The Boltzmann approach (Equation 10), which requires a suitably defined local equilibrium function f_α^{eq}. In Boltzmann network dynamics, f_α^{eq} is generally expressed as a series of powers of the global velocity:

$$f_\alpha^{eq} = A + Be_{\alpha i}u_i - Ce_{\alpha i}e_{\alpha j}u_i u_j + Du_i u_j \tag{13}$$

where: the Kronecker delta function δ_{ij} is:

$$\delta_{ij} = \begin{cases} 0, \text{ if } i \neq j \\ 1, \text{ if } i = j \end{cases} \tag{14}$$

The parameters of the local equilibrium function (15) must correspond to the following requirements.

$$\sum_{\alpha} f_{\alpha}^{eq}(x,t) = h(x,t) \tag{15}$$

$$\sum_{\alpha} e_{\alpha i} f_{\alpha}^{eq}(x,t) = h(x,t) u_i(x,t) \tag{16}$$

$$\sum_{\alpha} e_{\alpha i} e_{\alpha j} f_{\alpha}^{eq}(x,t) = \frac{1}{2} g h^2(x,t) \delta_{ij} + h(x,t) u_i(x,t) u_j(x,t) \tag{17}$$

An analysis of the lattice solution The Boltzmann equation (Equation 10) provides an approximation for the solution of the two-dimensional shallow water problem (Equation 5 and 6). The coefficients A, B, C, and D of Equation 13 were found by Mohamad (2011) based on conditions (15)–(17). The resulting local equilibrium function can be expressed as follows:

$$f_{\alpha}^{eq} = \begin{cases} h - \dfrac{5gh^2}{6e^2} - \dfrac{2h}{3e^2} u_i u_i, & \alpha = 0 \\ \dfrac{gh^2}{6e^2} + \dfrac{h}{3e^2} e_{\alpha i} u_i + \dfrac{h}{2e^4} e_{\alpha i} e_{\alpha j} u_i u_j - \dfrac{h}{6e^2} u_i u_i, & \alpha = 1,3,5,7 \\ \dfrac{gh^2}{24e^2} + \dfrac{h}{12e^2} e_{\alpha i} u_i + \dfrac{h}{8e^4} e_{\alpha i} e_{\alpha j} u_i u_j - \dfrac{h}{24e^2} u_i u_i, & \alpha = 2,4,6,8 \end{cases} \tag{18}$$

The use of the Chapman-Engkog approach demonstrates that the solution of the lattice Boltzmann Equation 10 using the equilibrium function (18) yields the solution of the shallow water Equations 5 and 6, where the components of force and viscosity are operationally defined as follows:

$$F_i = -gh \frac{\partial z_b}{\partial x_i} - \frac{\tau_{bi}}{\rho};\ \nu = \frac{e^2 \Delta t}{6} (2\tau - 1) \tag{19}$$

In accordance with Equation 10, it is necessary for the kinematic viscosity v to exhibit a positive value (Zhou, 2002).

$$\nu = \frac{e^2 \Delta t}{6} (2\tau - 1) > 0$$

Therefore, an acceptable limitation on the relaxation time is

$$\tau > \frac{1}{2}$$

Boundary conditions

The stability and precision in numerical simulations are highly dependent on boundary conditions. In the current study (Figure 3), the distribution functions, f_1, f_2 and f_8, at the lattice nodes along Line $\overline{AD}$ can't be predicted based on the values at the interior nodes. These parameters must be found by employing suitable boundary conditions. Based on empirical calculations, it has been observed that aligning the zero gradient of the distribution function with respect to the boundary is typically satisfactory. This implies that, following the process of streaming, the unknown value can be determined.f_1, f_2 and f_8 can be simply determined by

$$f_{\alpha}(1,j) = f_{\alpha}(2,j), \alpha = 1,2,8 \tag{20}$$

At the outflow border $\overline{BC}$, we can also have the following relations for f_4, f_5 and f_6

$$f_\alpha(N_x, j) = f_\alpha(N_x - 1, j), \alpha = 4,5,6 \tag{21}$$

where: N_x is the total x-direction lattice number.

Solid walls are assumed not to slip and the rebound scheme is applied. In the context of open boundaries, it is necessary to convert the criteria imposed on flow variables into conditions specific to distribution functions. One intrinsic challenge associated with the LBM approach pertains to the control of boundary conditions. Thus, conditions on velocities have been used at the entrance to the domain, while height h is kept constant at the domain exit Zhou (2002).

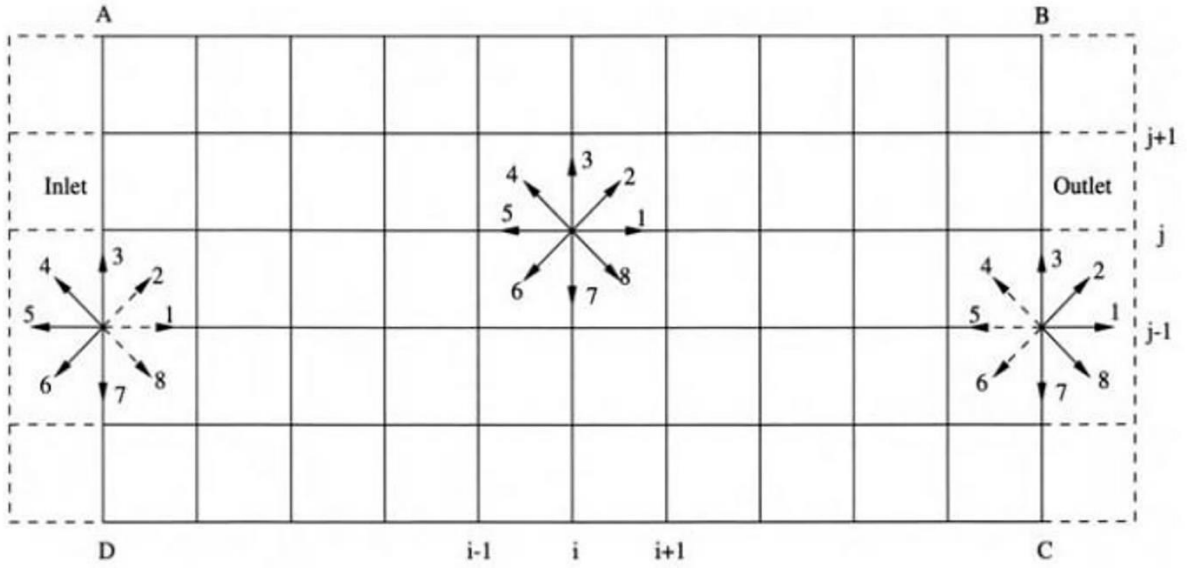

Figure 3. Inflow/outflow lattice nodes boundaries

The unknown distribution functions are obtained as follows:

$$f_0 + f_1 + f_2 + f_3 + f_4 + f_5 + f_6 + f_7 + f_8 = h \tag{22}$$

$$e(f_1 + f_2 + f_8) - e(f_4 + f_5 + f_6) = hu \tag{23}$$

$$e(f_2 + f_4) - e(f_6 + f_8) + e(f_3 + f_7) = hv \tag{24}$$

The three equations above for h, f_1, f_2 and f_8 are solved by :

$$f_1 = f_5 + \frac{2hu}{3e} \tag{25}$$

$$f_2 = \frac{hu}{6e} + f_6 + \frac{f_7 - f_3}{2} \tag{26}$$

$$f_8 = \frac{hu}{6e} + f_4 + \frac{f_7 - f_3}{2} \tag{27}$$

Sediment transport modeling

The granulometry of the bed material and flow conditions determine whether flowing water transports sediment particles as bed load or suspension load. Although bedload and suspension transfer are similar in nature, mathematical representation requires that a bed be defined with bedload transport. The concept of carriage refers to the transportation of particles through various mechanisms such as rolling, sliding, and saltation processes. Kalinske (1947) studied the trajectories and velocities of scavenged particles extensively. Einstein (1950), Bagnold (1956), and Van Rijn (1989) The present study examined the dynamics of charred particles by employing the equation of motion model for a saltant particle. Rouse proposed a universal equation that describes the equilibrium concentration

profiles of suspended sediments (1937). The equilibrium suspended sediment concentrations can be calculated as a function of depth above the bed using the following equation, provided that the particle fall velocity, sediment mixing coefficient, and reference concentrations are known. Rijn (1984) recommended the latter in terms of sediment characteristics and flow conditions.

Transportation of the bed load

The movement of particles along the bed surface under rolling and saltating action defines the bed load transportation. Defining (S_b) as the product of the particle velocity (u_b), the saltation height (δ_b) and the bed load concentration (c_b) resulting $S_b = u_b c_b \delta_b$ results. Van Rijn (1989) used numerical methods to solve the model for movement for a saltating particle and experimental data to explain S_b.

$$S_b = 0.053(\Delta g)^{0.5} d_{50}^{1.5} D_*^{-0.3} T^{2.1} \tag{28}$$

where:

$D_* = d_{50}\left(\frac{\Delta g}{\nu^2}\right)^{\frac{1}{3}} =$ particle parameter,

$T = \frac{(u_*')^2 - (u_{*,cr})^2}{(u_{*,cr})^2} =$ transport stage parameter,

$u_*' = (g^{0.5}/C')\bar{U} =$ the effective velocity of bed-shear,

$u_{*,cr} =$ the critical bed shear velocity as prescribed by Shields,

$\Delta = (\rho_s - \rho)/\rho =$ relative density,

$\rho_s =$ sediment density,

$\rho =$ fluid density,

$C' = 18\log\left(\frac{12h}{3d_{90}}\right) =$ Chezy coefficient corresponding to grains,

$\bar{U} = \sqrt{U^2 + V^2} \equiv$ depth-averaged velocity,

$d_{50} =$ particle size 50% of sediment mixture is finer,

$d_{90} =$ particle size 90% of sediment mixture is finer,

$\nu =$ kinematics viscosity coefficient,

$g =$ gravity acceleration.

Suspended load transport and equilibrium concentration profiles

The determination of the concentration profile under equilibrium conditions can be achieved by employing the simplified diffusion-convection equation as presented by Rouse.(Rouse, 1937) and solved by Van Rijn (1984) given as follow:

$$w_s c + \varepsilon_{s,z} \frac{dc}{dz} = 0 \tag{29}$$

In which,

$$\begin{aligned} \varepsilon_{s,z} &= \varepsilon_{s,\max}\left[1 - \left(1 - \frac{2z}{h}\right)^2\right] \text{ for } z < 0.5h \\ \varepsilon_{s,z} &= \varepsilon_{s,\max} \text{ for } z \geq 0.5h \\ \varepsilon_{s,max} &= 0.25\beta\kappa u_* h \end{aligned}$$

The equation mentioned before can be analytically integrated, resulting in,

$$\frac{c}{c_{a,e}} = \left[\frac{a}{z}\frac{(h-z)}{(h-a)}\right]^{\xi} \text{ for } z < 0.5h$$

$$\frac{c}{c_{a,e}} = \left[\frac{a}{(h-a)}\right]^{\xi} [e]^{-4\xi(z/h-0.5)} \text{ for } z \geq 0.5h$$

where: w_s – falling particle velocity, $\xi = \frac{w_s}{\beta \kappa u_*} =$ the parameter of suspension, κ – Von Karman constant, a – Reference level (Figure 4, little height above mean bed).

The equilibrium bed concentration is determined by the Van Rijn equation (Van Rijn, 1989) :

$$c_{a,e} = 0.015 \frac{d_{50}}{a} \frac{T^{1.5}}{D_*^{0.3}} \tag{30}$$

In which,

$$u_* = \text{ bed shear velocity } = g^{0.5}(U^2 + V^2)^{1/2}/C$$
$$C = \text{ Chezy coefficient } = 18\log(12h/k_s)$$

calculated equilibrium depth and integrated suspended sediment transfer as follows:

$$S_{s,x,e} = \int_a^h uc_e dz \text{ and } S_{s,y,e} = \int_a^h vc_e dz \tag{31}$$

where: $S_{s,x,e}$ – equilibrium x-direction suspended sediment movement, $S_{s,y,e}$– equilibrium y-direction suspended sediment movement, c_e – height-z equilibrium concentration (volume).

Bed level changes

In Figure 4, the sedimentary transport system is depicted, comprising a bed load layer with a thickness denoted as (a) and a suspended load layer with a thickness expressed as (h-a).

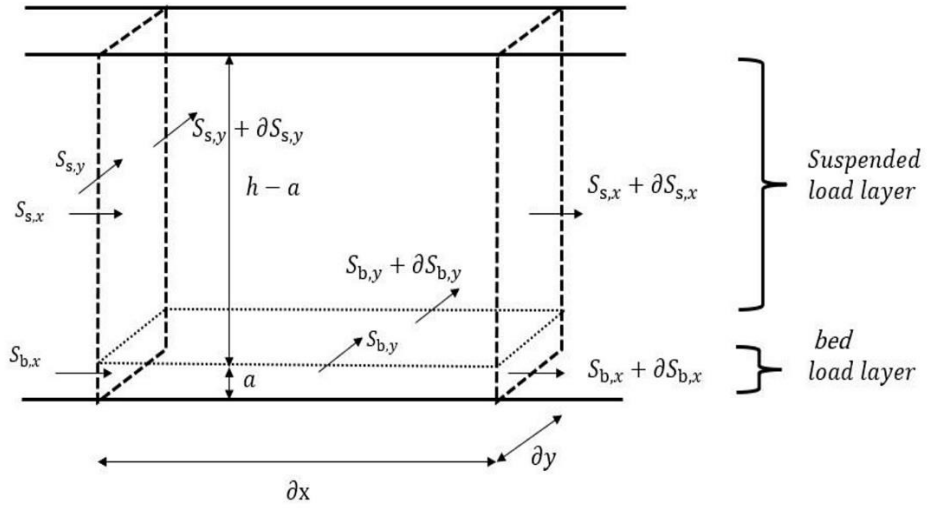

Figure 4. Sediment circulation scheme

The sediment mass balance formula is differentiated based on depth, leading to

$$\frac{\partial Z_b}{\partial t} + \frac{1}{1-p}\left\{\frac{\partial}{\partial x}(S_{t,x}) + \frac{\partial}{\partial y}(S_{t,y})\right\} = 0 \tag{32}$$

where: $S_t = S_s + S_b =$ depth-integrated transport of sediment, $S_s =$ depth-integrated suspended load transport, $S_b =$ bed-load transport, Equation 32 was solved using an explicit centered method. The discretized equation is:

$$R_{(i,j)} = \frac{z_{i,j}^{n+1} - z_{i,j}^{n}}{\Delta t} \tag{33}$$

$$\frac{z_{i,j}^{n+1} - z_{i,j}^{n}}{\Delta t} = \frac{-1}{(1-p)}\left[\frac{Q_{t,x}^{n}(i+1,j) - Q_{t,x}^{n}(i-1,j)}{2\Delta x} + \frac{Q_{t,y}^{n}(i,j+1) - Q_{t,y}^{n}(i,j-1)}{2\Delta y}\right] \tag{34}$$

where: $R_{(i,j)}$ – Rate of bathymetry changes (i,j) (mm/h), $Z_{(i,j)}$ – At all nodes, the bottom elevation Δt – Time step, $\Delta x, \Delta y$ – Space step,$Q_{t,x}$ – x-dependent component of total solid flow, $Q_{t,y}$ – y-dependent component of total solid flow.

Computational procedure

Present work proposes a hybrid technique to handle water flow and sediment transport concerns. Only the flow equations are solved using the LBM method, while the sediment transport and bottom evolution equations are calculated using FDM. LBM and FDM coupling are used in the following calculations. Thus, for fluid flow and sediment transport problems, water depth and velocity have related effects. Consequently, this method requires the execution of both LBM and FDM. After defining the initial conditions, LBM solves the velocity field with the initial water depth. Next, the solid flow rates are calculated using the velocities obtained with LBM. Solution of the solid mass conservation equation (Equation 10) above calculates bottom elevation change rate. The computations were done in a 1000 m wide, 3100 m long rectangular channel with a horizontal bed. The channel is partially confined by a 400 m long, 100 m wide dam.

The solution methodology for the hybrid model is direct and can be stated as follows. Provided the initial water depth and velocity:

1. f_α^{eq} is calculated from Equation 18,
2. f_α is determined from Equation 10,
3. The water depth and velocity are updated by Equations 11,
4. Next time step, use the normal LBM algorithm and go back to step 2 until you get a permanent hydrodynamic field.
5. Using the fluid velocity u and water depth h from step (3) to compute the bedload and suspension load (Equations 28 and 31)
6. Evaluate the new bottom evolution by solve Equation 32.

Diagram of the mesh adopted

A network of 310 points with a y-direction dimension of 100 points illustrates the dam. The LBM solutions were derived using a 10 m network resolution size (Δx = Δy). The left open boundary has a uniform velocity u = 0.66 m/s, while the left open flow boundary has a constant water depth of 6 m (Figure 5).

RESULTS AND DISCUSSION

This section will be divided into two subsections, the first will be devoted to model validation, while the model's ability to handle more geometrically complex cases will be highlighted in the second sub-section, The present study aims to examine the impact of different impediments on the dynamics of flow and sediment.

Model validation

The model developed was applied to an industrial case already studied by (Charafi et al., 2000). This requires performing a numerical validation of the current model through a comparison of its results with those of Charafi's model. The hybrid model employed in this study utilizes LBM in the hydrodynamic module and FDM in the solid transport module, incorporating a well-defined central scheme. The precision and numerical robustness of flow predictions using LBM are highly dependent on the selected collision operator. The BGK collision term, in conjunction with a bounce-back approach to boundary conditions, is extensively

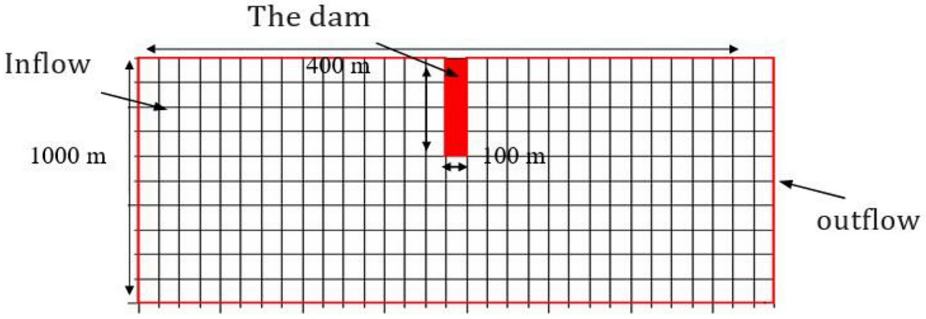

Figure 5. Schematic description of channel with a dam (inflow and outflow boundaries)

utilized in the simulation of fluid flows through the application of the LBM.But when encountering huge velocity gradients, this model's heavy reliance on a singular relaxation time inherently imposes its numerical stability. Moreover, it is well-established that the absence of invariance in the standard LBM presents numerous difficulties when attempting to simulate high-velocity flows. This also enables the examination of the stability of the hybrid approach.

As a consequence, only diffusion-convection will be evaluated by the DFM solver and the LB relaxation time is set to $\tau = 0.78$. The model developed by (Charafi et al., 2000) is based on the use of FDM with a Maccormack scheme used in the hydrodynamic module, and an explicit center scheme in the solid transport module. In order to provide numerical stability at high-dimensional numbers, the LBM scheme requires a larger number of grid positions compared to the FDM. Additionally, as the grid refinement grows, the LBM scheme necessitates a higher number of time steps.

Hydrodynamic module validation

The depth-averaged flow velocity field derived using the LBM model described above is depicted in Figure 6. The acquired results exhibit a high level of concurrence with the findings reported by

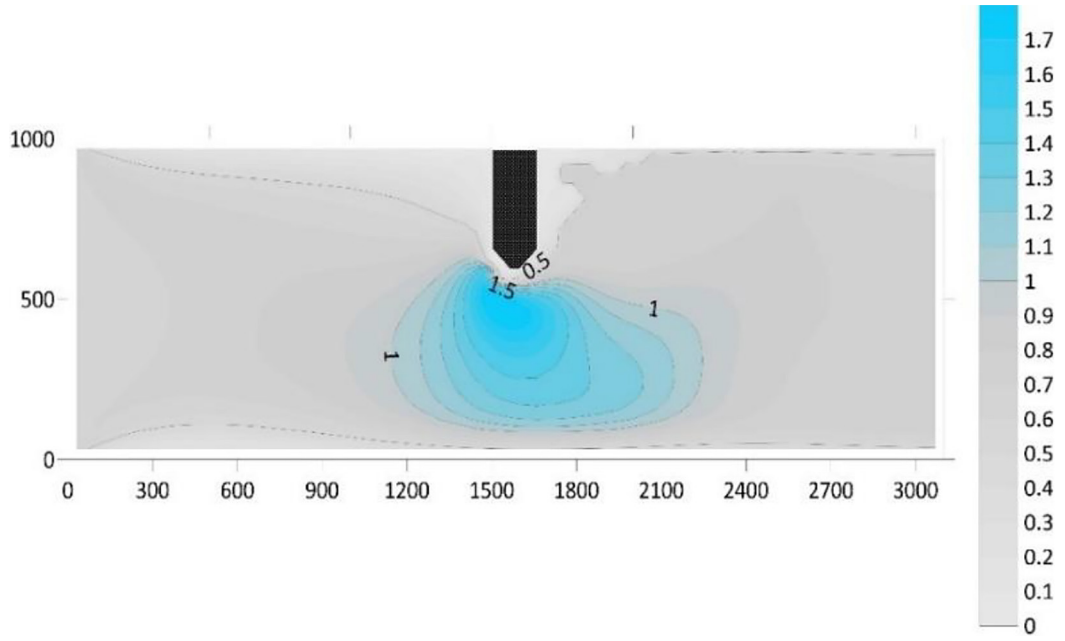

Figure 6. Flow velocity field (m/s) based on LBM

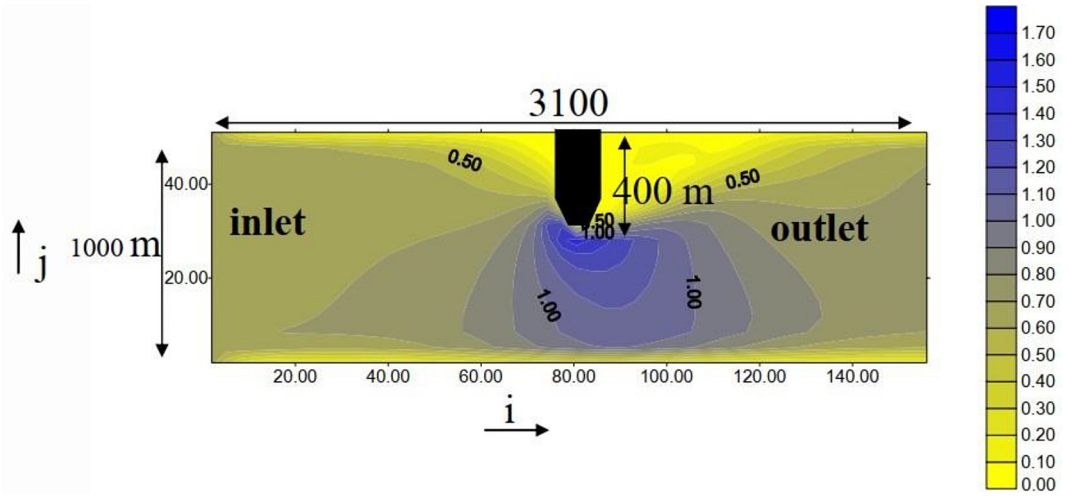

Figure 7. Flow velocity field (m/s) based on MacCormack scheme (Charafi et al., 2000)

(Charafi et al., 2000) (Figure 7), who employed the McCormack scheme (Bernsdorf et al., 1999; Charafi et al., 2000). The findings are derived using a Manning coefficient of n = 0.032 s/m$^{1/3}$, and the relaxation time τ of the LBM approach has been assumed to be 0.78. In close proximity of the dam head, the channel indicates a maximum flow velocity of 1.70 m/s. We merge the horizontal velocity components with vertical logarithmic profiles to generate a three-dimensional hydrodynamic field. This work simply identifies the quasi-tridimensional model as such.

Validation of the sediment transport module

With regard to the sediment transport module, Figures 8 and 9 show a comparison of this study's results achieved through the current approach with those reported by (Charafi et al., 2000). The numerical results presented in Figure 8 illustrate the spatial distribution of suspended solid flow along a channel, based on the equilibrium approach, showing a maximum flow $q_{s,e}$ near the dam head. This flow rate of 32 kg/sm (Figure 8) has a high level of concurrence with the findings presented in (Charafi et al., 2000) (Figure 9). Hence, the

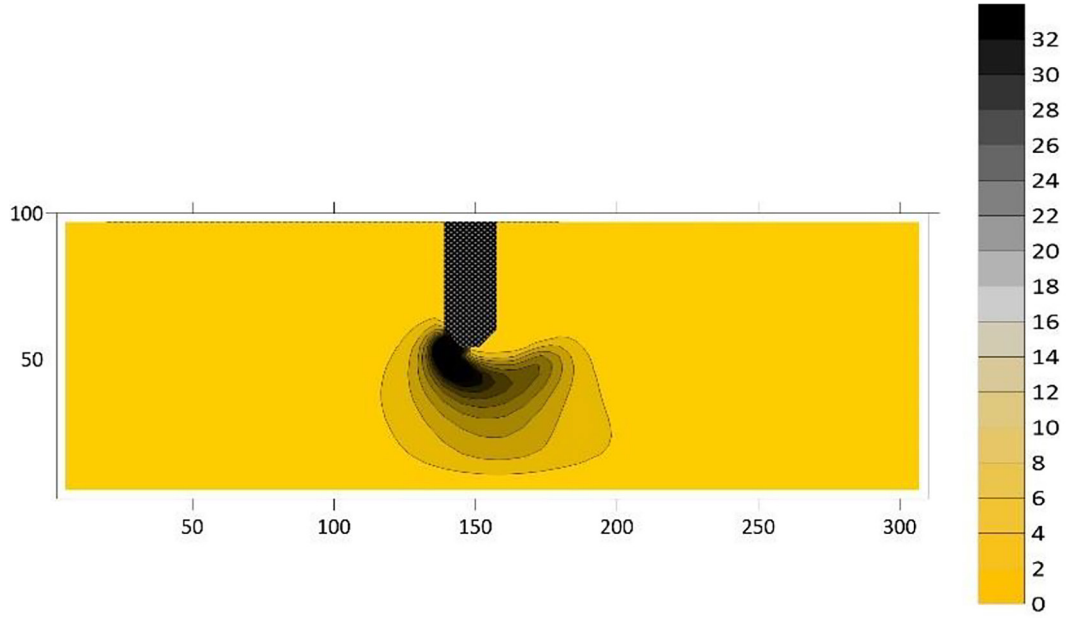

Figure 8. Equilibrium suspended sediment transport distribution (kg/sm)

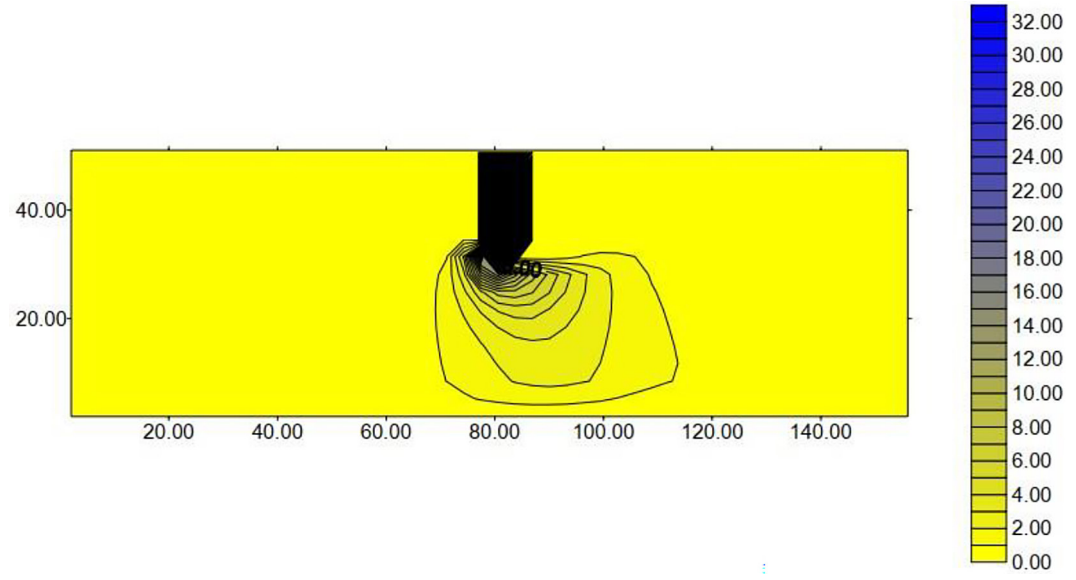

Figure 9. Distribution of suspended sediment transport in a state of equilibrium (kg/sm) (Charafi et al., 2000)

findings are qualitatively consistent with the research conducted by (Charafi et al., 2000).

The evolution of the bed change profiles in Figures 10 and 11 exhibits a high level of concurrence between the findings of the current study and those reported by (Charafi et al., 2000). The erosion rate depicted in Figure 10 exhibits a peak value of around 700 mm per hour at close proximity to the dam head. The findings presented in this study exhibit a high level of concurrence with the results reported by (Charafi et al., 2000) (Figure 11). A strong concurrence was seen between the findings of the current study and the results reported by (Charafi et al., 2000) demonstrates once again the efficiency of the computational code developed, and its ability to predict other industrial cases, which gives us the ambition to use our computational code to handle other cases with more complex configurations, which was the subject of the simulations presented in the rest of this work.

Application of the hybrid model – effect of different dikes arrangements

After having validated our model, we are now interested in its application to more complex cases. We consider the flow in the same channel but this time equipped with several obstacles in the form of dikes (Figure 12). Several scenarios will be simulated, focusing on the influence of

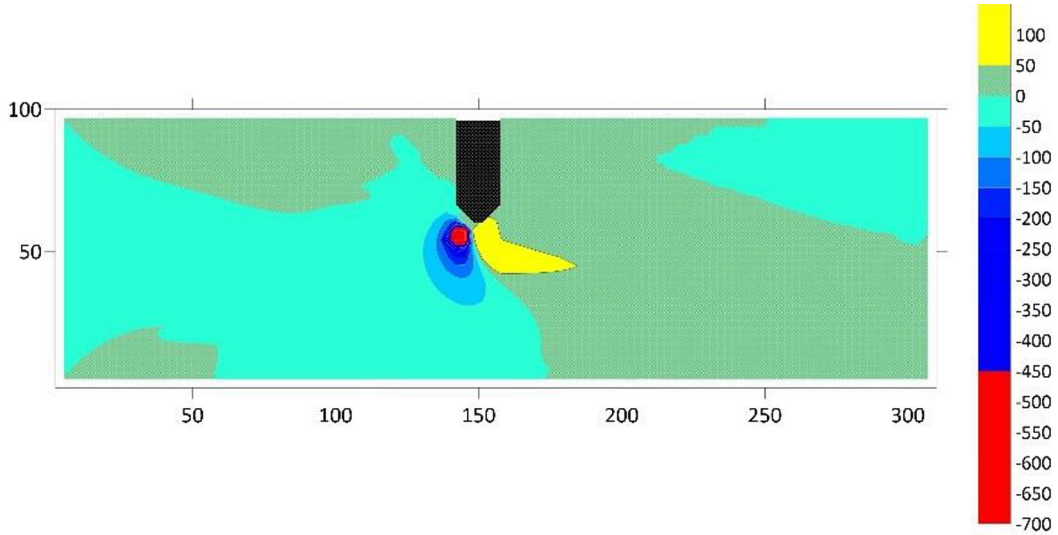

Figure 10. The bed change rate (mm/h) is calculated using equilibrium transport (present work)

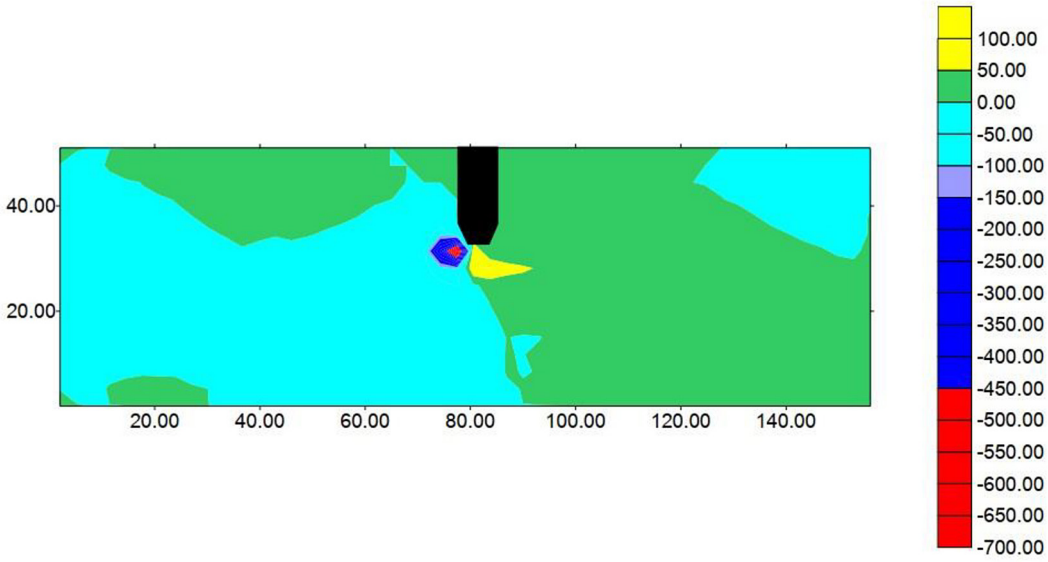

Figure 11. The bed change rate (mm/h) is calculated using equilibrium transport (Charafi et al., 2000)

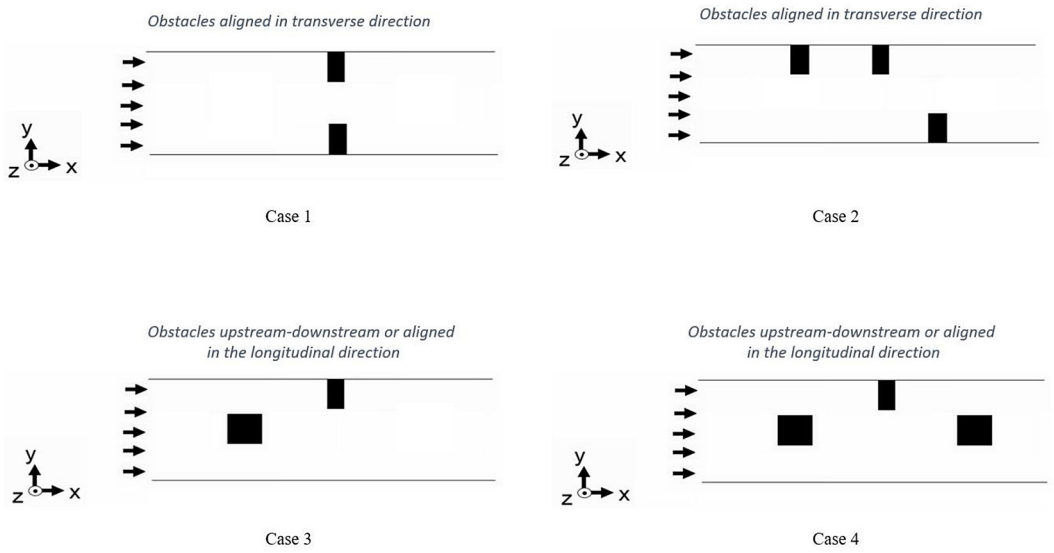

Figure 12. Studied cases – different dykes arrangements

different obstacle arrangements on hydrodynamic profiles, sediment fluxes and the evolution of channel bottom change rates. The interest in considering such configurations is on the one hand to confirm the capacity of the developed code to simulate complex cases, and on the other hand to understand the complex phenomenon of solid transport in the presence of structures in the canal.

Depending on the number of obstacles in the channel, their position, size and spacing, multiple effects may appear. The four figures below illustrate the obstacles considered. The complexity of the physical phenomena involved in flows following a multitude of obstacle arrangements justifies the development of our hybrid model in the present work, where the LBM method proves effective in simulating velocity fields for this type of configuration (Figure 13).

Effects of obstacles on the hydrodynamic field

Our simulations examined four examples to analyze the impact of obstacles located centrally in

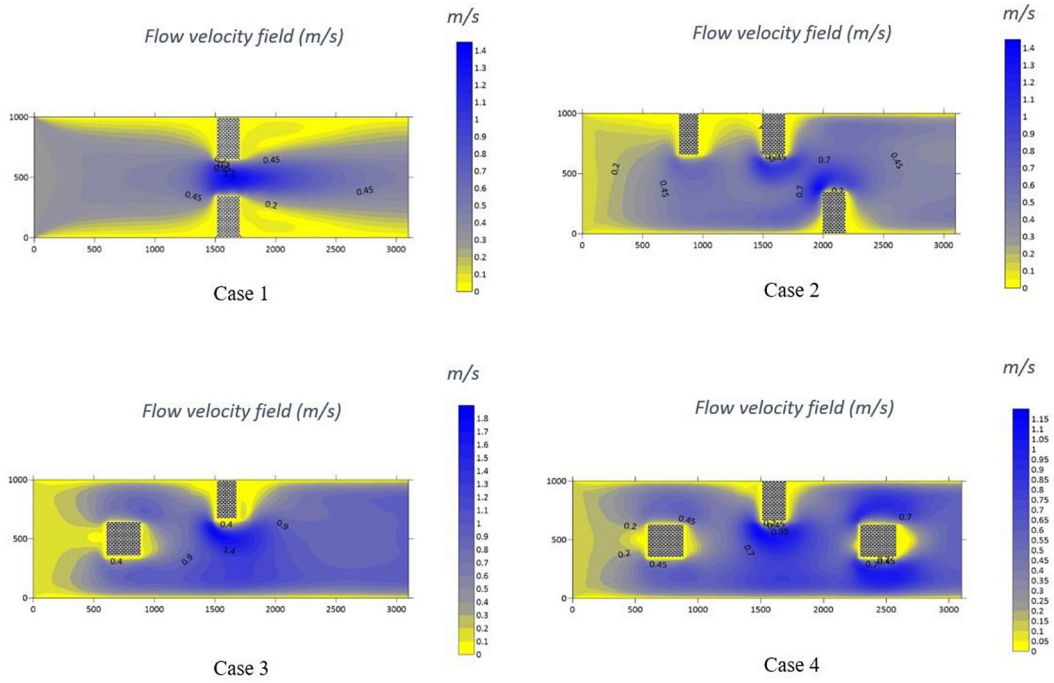

Figure 13. Flow velocity field (m/s)

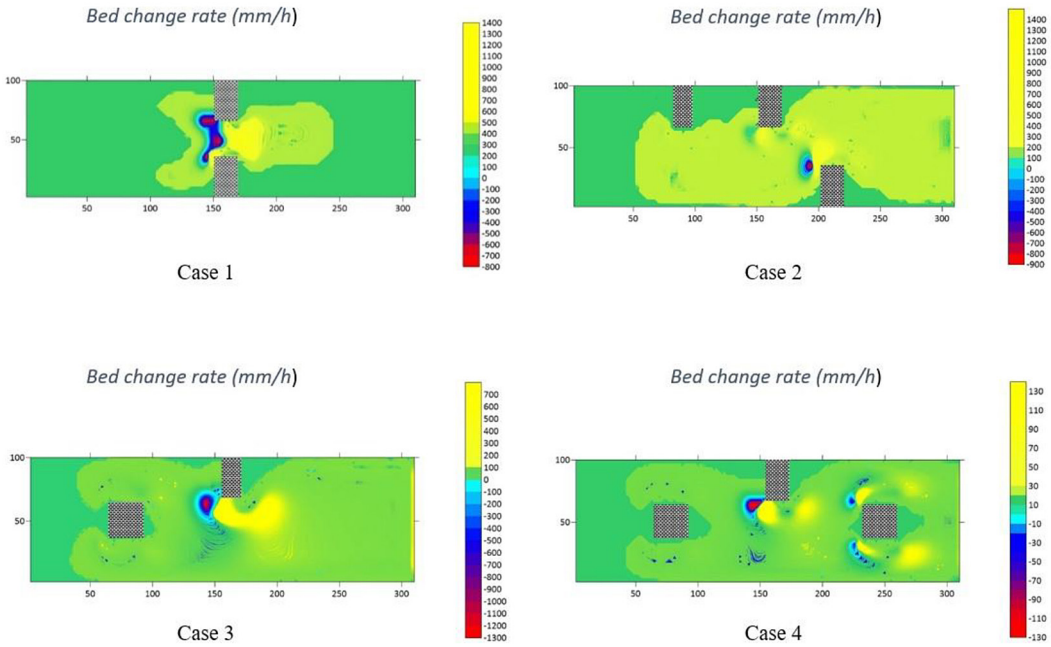

Figure 14. Rate of bed change (mm/h)

the channel and borders it horizontally. The results clearly demonstrate that these obstacles significantly affected the flow regime. Indeed, the results indicate a reduced velocity of fluid flow before the obstacle is present compared to the velocity observed after the obstruction. This creates an area of swirling water accumulation before the obstruction and a region of turbulent flow after the obstruction. The area of the obstacle's zone of influence is contingent upon its dimensions, configuration, and placement. Furthermore, the dikes along the banks of the channel resulted in the formation of vortices and localized variations in velocity.

On the other hand, the effect caused by the dikes reducing the width of the channel has created narrowing zones where the flow of water is forced into a narrower space, causing an increase in the speed of the water in the areas between the dikes, and verifies the continuity equation. This would explain the appearance of erosion zones following the increase in shear stresses thus exceeding the critical erosion stress. The hydrodynamic results therefore allow us to predict the impact of local variations in water speed, which can lead to erosion processes in high-velocity areas and sediment deposition in low-velocity areas.

Sediment profile in the presence of dykes

To forecast the regions affected by erosion and deposition, we employed the outcomes of the identical scenarios examined in the hydrodynamic module to compute the velocity of solid flows and then forecast the progression of the lower stratum within the channel. Based on the case studies depicted in Figure 14, it can be observed that the hydrodynamic field has a direct impact on the mass balance and subsequently on the evolution of the bed bottom, aligning with the expected result. High velocity areas give rise to large solid flows, while small solid flows result from low velocities. Thus, the balance of what enters and exits locally in each area of the channel (or control volume in the sense of finite difference discretization) gives rise to erosion or deposition before, after and near obstacles. As a result, bed bottom change rates result in changes in channel bathymetry. Furthermore, the intensity of these rates of change is clearly related to the intensity of the hydrodynamic field, based on the positioning of obstacles and dikes presented in the four different channel cases. It should be noted that solid flows are obtained by adding bottom and suspension solid flows.

The obtained results demonstrate the code's ability to evaluate the impacts of specific obstacles in each given context. These results, therefore, allow for proactive management and engineering measures. In order to have a greater understanding of the impacts of obstacles, it may be important to consider erosion and deposition rates in the channel.

CONCLUSION

In order to forecast alterations in bed levels within a channel that is equipped with dikes, a quasi-three-dimensional sediment transport model has been constructed. The present model involves the computation of flow velocities, sediment concentration profiles, depth-integrated sediment transport rates, and initial bed level variations through the utilization of an equilibrium transport equation.

The developed computational code is hybrid, combining the lattice Boltzmann method for the hydrodynamic part and the finite difference method for sediment dynamics. The efficiency and simplicity of applying the lattice Boltzmann method to simulate free-surface flow hydrodynamics, combined with the complexity of solid transport phenomena, motivated the adoption of a hybrid model. This hybrid nature allows for realistic simulations by coupling hydrodynamics, solid transport, and bed level changes in an unsteady manner. The obtained results show that the presence and arrangement of dikes influence flow velocities, increasing them in constricted areas, which leads to erosion due to shear stresses exceeding the critical bed erosion stress. Conversely, deposits form in low-velocity eddy zones behind the dikes, where stresses are below the critical bed deposition stress, validating the model for complex cases. The validation of the code was successfully achieved through original simulations, such as modeling flow with various dike configurations in a channel. These simulations demonstrated the code's ability to provide credible results even for intense flow conditions. Finally, the importance of experimentation remains crucial. Numerical advancements cannot replace the fundamental understanding of phenomena and the establishment of precise empirical relationships. Improved friction laws and generalized transport capacity laws directly impact the quality of numerical simulations. Experimental results are increasingly relevant and can be better utilized with a functional and efficient simulation code, enhancing their pertinence and utility.

REFERENCES

1. Adamsson Å., Lars V.B. 2003. Bed shear stress boundary condition for storage tank sedimentation. Journal of Environmental Engineering, 129(7), 651–658.
2. Aidun C.K. and Clausen, J.R 2010. Lattice-boltzmann method for complex flows. Annual review of fluid mechanics, 42, 439–472.
3. Bagnold R.A. 1956. The flow of cohesionless grains in fluids. Philosophical Transactions of the Royal Society of London. Series A, Mathematical and Physical Sciences, 249(964), 235–297.
4. Benkhaldoun F.E., Mohammed I.S. 2007. Well-balanced finite volume schemes for pollutant transport by shallow water equations on unstructured meshes. Journal of computational physics, 226(1), 180–203.
5. Bernsdorf J., Durst F., Schäfer M. 1999. Comparison of cellular automata and finite volume techniques for simulation of incompressible flows in complex geometries. International Journal for Numerical Methods in Fluids, 29(3), 251–264.
6. Bhatnagar P.L., Gross E.P., and Krook M. 1954. A Model for collision processes in gases. I. Small Amplitude Processes in Charged and Neutral One-Component Systems. Physical review, 94(3), 511.
7. Brush S.G. 2003. Kinetic theory of gases, The: an anthology of classic papers with historical commentary. World Scientific.
8. Cai L.X., Feng W.-X., Zhou J.-H. 2007. Computations of transport of pollutant in shallow water. Applied Mathematical Modelling, 31(3), 490–498.
9. Charafi M.M.S., Kamal A A. and Menai, A. 2000. Numerical modeling of water circulation and pollutant transport in a shallow basin. International Journal of Modern Physics C, 11(4), 655–664.
10. Charafi M.M.S., Kamal A.A, and Menai, A. 2000. Quasi-three-dimensional mathematical modeling of morphological processes based on equilibrium sediment transport. International Journal of Modern Physics C, 11(07), 1425–1436.
11. Chen S. and Gary D.D. 1998. Lattice boltzmann method for fluid flows. Annual review of fluid mechanics, 30(1), 329–364.
12. Einstein H.A. 1950. The Bed-Load Function for Sediment Transportation in Open Channel Flows. US Department of Agriculture.
13. Gawas A.S. and Dhiraj V.P. 2021. Axisymmetric lattice boltzmann formulation for mixed convection with anisotropic thermal diffusion and associated bubble breakdown. Physics of Fluids, 33(3).
14. Guo Z. and Chang S. 2013. Lattice Boltzmann method and its application in engineering. World Scientific.
15. Hu C.J., Guo, Q.Z. 2010. Flow movement and sediment transport in compound channels. Journal of Hydraulic Research, 48(1), 23–32.
16. Kalinske A.A. 1947. Movement of sediment as bed load in rivers. Eos, Transactions American Geophysical Union, 28(4), 615–620.
17. Klar A.S., Guido M.T. 2008. Lattice boltzmann simulation of depth-averaged models in flow

hydraulics. International Journal of Computational Fluid Dynamics, 22(7), 507–522.

18. Mohamad A.A. 2011. Lattice Boltzmann Method. Springer.
19. Rijn, L.C. 1984. Sediment transport, part II: Suspended load transport. Journal of hydraulic engineering, 110(11), 1613–1641.
20. Van Rijn L.C. 1989. Mathematical Modelling of Morphological Processes in the Case of Suspended Sediment Transport.
21. Rouse H. 1937. Modern conceptions of the mechanics of fluid turbulence. Transactions of the American Society of Civil Engineers, 102(1), 463–505.
22. Shi Y. and Xiaowen S. 2021. A multiple-relaxation-time collision model for nonequilibrium flows. Physics of Fluids, 33(3).
23. Suzuki K.I., Nakamura T., Horai A., Pan F., Masato K.-L.Y. 2021. Simple extended lattice boltzmann methods for incompressible viscous single-phase and two-phase fluid flows. Physics of Fluids, 33(3).
24. Balam R.I., Nguyen K.D., Salazar L.G., Zapata M.U. 2021. An unstructured finite-volume semi-coupled projection model for bed load sediment transport in shallow-water flows. Journal of Hydraulic Research, 59(4), 545–558.
25. Wen M., Li W., Zhao Z. 2022. A hybrid scheme coupling lattice boltzmann method and finite-volume lattice boltzmann method for steady incompressible flows. Physics of Fluids, 34(3).
26. Wu B., Zhang B., ShiY., Li S. 2021. Large eddy simulation of sediment transport in high flow intensity by discrete particle method. Journal of Hydraulic Research, 59(4), 605–620.
27. Zhou J.G. 2002. A lattice boltzmann model for the shallow water equations with turbulence modeling. International Journal of Modern Physics C, 13(08), 1135–1150.
28. Zou Q. and He X. 1997. On pressure and velocity boundary conditions for the lattice boltzmann BGK model. Physics of fluids, 9(6), 1591–1598.